



DESIGN AND ANALYSIS OF A DYNAMIC STRUCTURE FOR THE STUDY OF MULTIPHASE FLOW INDUCED VIBRATION

Ricardo P. Álvarez

Fabio Kanizawa

Gherdhart Ribatski

Leopoldo P. R. de Oliveira

Departament of Mechanical Engineering

São Carlos School of Engineering

University of São Paulo

Av. Trabalhador Sancarlense 400

13566-590 São Carlos, SP, Brazil

ricardo.alvarez@usp.br

fabio.t.kanizawa@gmail.com

ribatski@sc.usp.br

leopro@sc.usp.br

Abstract. *Flow-Induced Vibration (FIV) in tube bundles is an important issue in the design of heat exchangers, due to the potential damage that may result from it. Many test benches have been constructed to study the flow-structure interactions that occur in those equipments, however, some vibration mechanisms, mostly those related to multiphase flow, are not yet fully understood. Therefore, in this work, the design and analysis of a dynamic device consisting of an instrumented flexibly suspended tube for the study of the FIV are presented. The function of this system is to allow the suspended tube to vibrate under the excitation of multiphase flow, as part of a tube bundle test bench that represents a steam generator of a nuclear plant. Several suspension devices used in FIV studies have been reviewed as well as academic and real systems were considered during the conceptual design phase. Based on the literature review and the particular features of the complete test bench currently under construction, a wire system solution is devised and constructed. This paper also presents some preliminary tests carried out on the dynamic subsystem, aiming at addressing the mode shapes and resonance frequency range provided by the proposed suspension. The results are compared with data of previous FIV experimental studies.*

Keywords: *flexible mounted tube, flow-induced vibration, multiphase flow, resonance frequency*

1. INTRODUCTION

Since the 1960's, when critical failures in nuclear power plants equipments began to appear (Paidoussis, 1982) and engineers realized the lack of knowledge of flow-induced vibration (FIV) for equipments design, considerable progress has been made in obtaining a better understanding in fluid-structure interaction in heat exchangers tube bundles and similar devices subjected to external cross-flow. From those days, different test benches were constructed and several experiments were performed to understand the causes of vibration in tube bundles. As a result, it is possible nowadays to recognize, in a relatively good manner, the main FIV mechanisms for single-phase cross-flow. A review of this progress is described in detail by Paidoussis (1982), also a theoretical analysis can be found in Blevins (1977). After that, due to the fact that phase change occurs in most of these heat exchangers, the attention came over multiphase flow-induced vibration in tube bundles where, according to Goyder (2002), almost the same vibration mechanisms seen in single-phase flow test appear. However, the tube response in multiphase flow is not fully understood yet which is not a surprise because of the complexity involved in multiphase fluid-structure interactions. In both, multi and single-phase cases, vibrations were measured by an instrumented tube surrounded by other tubes in a test section, which represents a real tube bundle. Khushnood *et al.* (2004) present a review of representative published tests on two-phase flow across tube arrays, nevertheless, details about the mounted tube configuration were not mentioned. In all those researches, many configurations were used to suspend the instrumented tubes across the test section; the more representative will be outlined below.

One of the most common methods to fix tubes in a test section is to mount it in a cantilever configuration with a highlight to the study of Axisa *et al.* (1990), that focused on the study of turbulent buffeting FIV mechanism due to single and two-phase cross-flow. The used test array configuration is composed by all clamped - clamped tubes except one that was clamped - free installed. Accelerometers and strain gauges were installed on the flexibly mounted tube to measure its response. It was used different tubes for air and water tests, the natural frequencies measured were 33 Hz and 109 Hz respectively.

Another experimental study performed in a similar test bench is presented in Pettigrew *et al.* (2001). This work was focused on the influence of the tube bundle geometry in fluid-elastic instability, turbulent buffeting, damping and

hydrodynamic mass phenomena for countergravity two-phase cross-flow. Two types of experiment were conducted; in the first one the test section was composed by an all cantilevered tube bundle, with each tube natural frequency of roughly 30 Hz that, according to the authors, is typical for heat exchanger tubes. For the second test a unique flexible tube surrounded by clamped - clamped tubes was used. This variation was made to avoid hydrodynamic coupling effect between tubes and allowed the study of damping and turbulent buffeting excitation. The new natural frequency for the “rigidly” mounted tubes changed to 160 Hz.

Tubes in test section have been already used as force transducers, as presented in Zhang *et al.* (2008). In this research a model to correlate vibration excitation forces to dynamic characteristics of two-phase cross-flow in a cylinder bundle is developed. For that, a single flexible cylinder is appropriately instrumented with strain gages to measure drag and lift forces. As in previously cited studies, this cylinder is surrounded by rigid non instrumented cylinders. Due to the fact that the instrumented cylinder natural frequency was higher than excitation force frequencies, higher than 150 Hz, this cylinder functioned as a dynamic force transducer.

Based on the above mentioned studies, it can be concluded that a flexible tube configuration can be used for analysis of FIV during single and multiphase flow. Additionally, this approach has the advantage of being easier to be designed and constructed. However, a clear disadvantage is that its natural frequency cannot be modified *in situ*. Actually, to modify it would be necessary to change tube dimensions or materials. Furthermore, if a structural dynamic analysis of the instrumented tube is needed, the cantilever device may introduce some problems in experimental and model results contrast. To avoid these circumstances, in many cases a dynamic structure to suspend the instrumented tube across the test section is used.

Grover and Weaver (1978) performed a study of FIV due to single-phase cross-flow using a dynamic structure for mounting tubes in test section. The authors installed a tube bundle with 138 tubes in the cross section of a horizontal wind tunnel. The bundle had 19 tubes that were flexible suspended by a dynamic structure composed by: tensioning devices, piano wires and an oil damper. The main function of this structure is to enable the tuning of tubes natural frequency just by stretching the piano wires, therefore it is not necessary to change neither tubes material nor geometry. Tube natural frequencies were obtained in the range of 18 - 25 Hz. Due to the necessity of studying fluid-elastic instability and vortex shedding occurring distinctly in the same test array a discrete device like the viscous damper was introduced. Thus, tuning the tube natural frequencies and introducing damping to the dynamic structure would help to have a wider range of tests.

A similar test bench is used in Price *et al.* (1987), which main objective was to study the FIV phenomena in a rotated square array of rigid cylinders with a 2.12 pitch-to-diameter ratio (P/D). In this study, tests for water and air flows were performed separately; different dynamic structures to suspend the instrumented tubes were used. For air cross-flow tests a tunnel was used, the instrumented tubes were suspended by tensioned piano wires and damping is introduced by a viscous discrete device as in Grover and Weaver (1978). Also it is mentioned that the frequency range of interest is between 0 - 25 Hz, therefore the tube natural frequency range must cover this range. Based on the test bench description, that is available in this document, the only different feature in relation to the Grover and Weaver (1978) test bench was the introduction of a mechanism to avoid the change of the tube equilibrium position due to drag forces. This device was included with the aim of preventing a local change of the pitch-to-diameter parameter. On the other hand, for the water flow test, the instrumented tube that pans the test section was attached at its lower end to a thinner brass tube mounted in cantilever in the tunnel wall; thus this structure functions as a flexible support that permits tube displacements. According to Grover and Weaver (1978), no efforts were made in order to avoid blowback displacement, due to the fact that these devices were not compatible with sealing elements.

As it can be noticed from the above discussion, using a dynamic structure to suspend the tubes could be very useful since natural frequencies can be tuned to values that allow analysis of parameters that affect stability boundaries like fluid-elastic instability, or even to create conditions that allow the analysis of turbulent excitation. As a result of the facts above, a wire dynamic subsystem have been designed, constructed and tested to evaluate if it can be used for multiphase FIV researches in a test bench currently under construction. This paper presents the design and tests in the dynamic subsystem. Experimental results are presented for air, water and multiphase stagnant conditions.

2. EXPERIMENTAL APPARATUS

2.1 Subsystem set-up

A dynamic subsystem is designed and constructed to perform experiments aiming at addressing the mode shapes and resonance frequency range provided by the dynamic structure that will be used for tube suspension in a test bench currently under construction. A picture of the subsystem is presented in Fig. 1. It is composed by a frame made of aluminium L-profiles with overall dimensions: 770 mm long, 250 mm wide and 250 mm height; two slide devices; four guitar tuners, four steel wires 0.4 mm diameter; two designed devices to host the accelerometers and stainless steel tube 415 mm long, 19 mm outside diameter and 2 mm wall thickness. The four guitar tuners are attached at the ends of the frame larger dimension, their position must allow tube vibration in a horizontal or vertical plane in the middle of the frame. The accelerometers hosts are introduced in the tube, both axial and angular relative displacements between those parts are

avoided using bolts. Finally the tube subassembly is suspended by two parallel mounted tensioned steel wires. Thus, tube resonance frequencies can be modified by stretching the wires using the guitar tuners. The first resonant frequency is used as a reference value to tune the tube. Just as a functionality experiment, tests for different force amplitudes were performed to confirm the linearity. By using the same wire tension level equal Frequency Response Functions (FRF) were obtained. Therefore, wires can be assumed linear stiffness springs.

Moreover, an acrylic reservoir has been filled for water environment tests. The water level is at least 7 cm above the tube axis as it is presented in Fig. 2 and Fig. 3. For the multiphase case an air injector has been submerged in the stagnant water to generate small (up to 1.5 mm diameter according to the supplier) and relatively well distributed bubbles. The experiment including the air injector can be seen in Fig. 4. An air pressurized facility is used to feed the injector. The air flow is controlled with a needle valve and measured with a turbine flow meter.

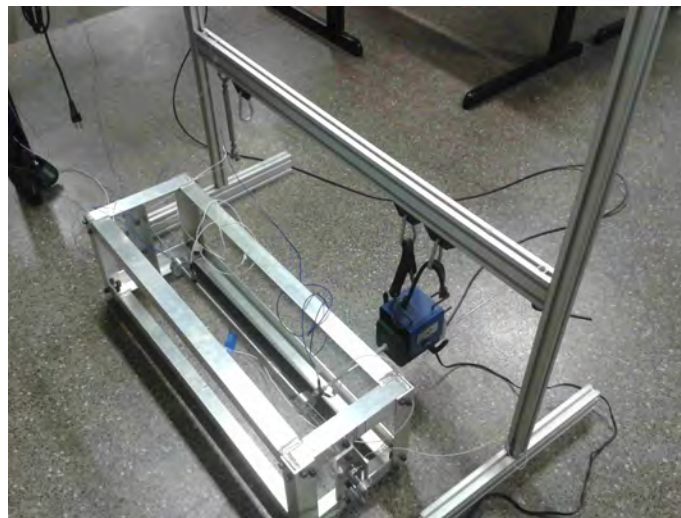


Figure 1. Test set - up for tests in x direction - air environment.

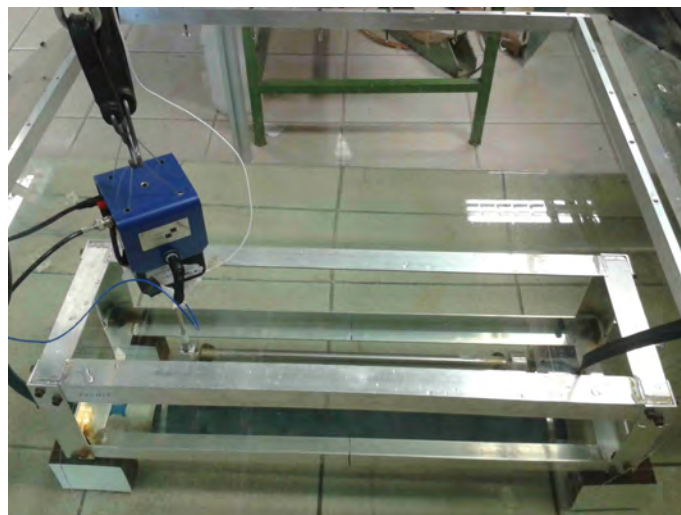


Figure 2. Test set - up for water environment.

2.2 Instrumentation

The dynamic subsystem is excited with an electrodynamic shaker model K2007E01 from Modal Shop. Force and acceleration are measured with an impedance head model 288D01 from PCB Piezotronics, it is installed at the force application point, this set - up is presented in Fig. 5 for a x coordinate excitation. For the air environment case, the impedance head is mounted directly between the stinger and the tube. For the water and multiphase environment cases, the impedance head is set next to the shaker. Additionally, microaccelerometers model 352A24, also from PCB Piezotronics, are installed inside the tube just for air environment cases. Data is acquired with a LMS SCADAS Mobile system running LMS Test.Lab.

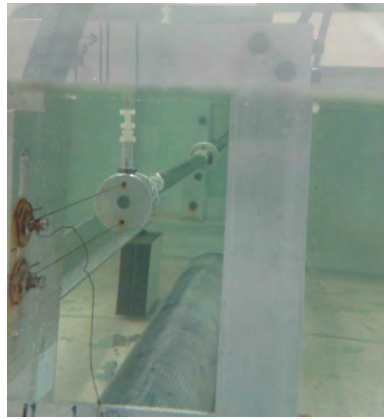


Figure 3. Shaker set - up for y coordinate tests in water environment.



Figure 4. Test set - up for multi - phase environment.

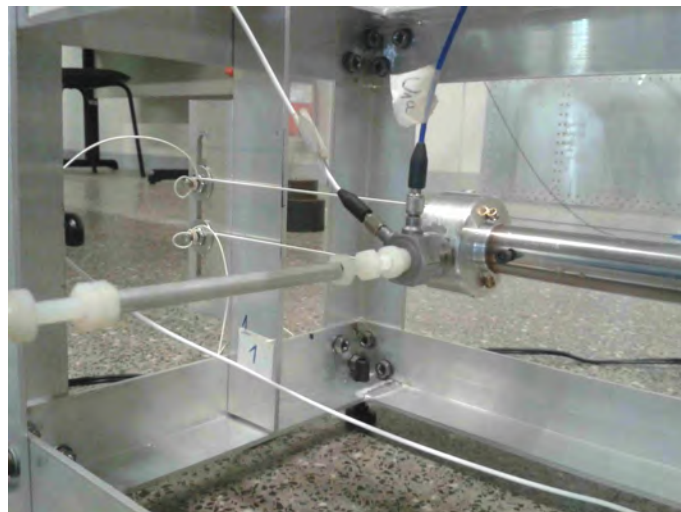


Figure 5. Impedance head setup for x coordinate excitation.

3. EXPERIMENTAL RESULTS

Vibration tests were performed in the subsystem detailed above. The tube was excited in x and y coordinates in air, water and multiphase environment. As a first group of experiments, aiming at recognizing the system dynamic behavior, tests were made for different wire tension levels in air environment, FRFs plots are presented in Fig. 6 and Fig. 7. In both x and y excitation tests, two resonance frequencies appeared within the 0 - 256 Hz frequency bandwidth. As it can

be noticed from the FRFs, the higher the tension in the wires the higher the tube resonance frequencies, which can be seen as the peaks are shifted to the right. Furthermore, Tab. 1 and Tab. 2 show that for different tension cases the ratio of the second to the first resonance frequency is maintained. Sinusoidal excitation with each resonance frequency was conducted in two different experiments to identify the mode shapes. Visual observation showed that the first mode shape corresponds to a bouncing displacement in the coordinate of excitation and the second one is to tube rocking mode. For the next experiments, the first resonance frequency in air in the x direction is used as a reference value to tune the system, the adopted value is of 11 Hz.

Table 1. Tube resonance frequencies under x direction excitation obtained for different wire tension levels in air environment.

Tension level (ascending order: 1 to 4)	1	2	3	4
First resonance frequency (Hz)	10.25	10.50	12.5	14
Second resonance frequency (Hz)	18.75	19.5	22.25	25.5
Frequencies ratio	1.83	1.86	1.78	1.82

Table 2. Tube resonance frequencies under y direction excitation obtained for different wire tension levels in air environment.

Tension level (ascending order: 1 to 4)	1	2	3	4
First resonance frequency (Hz)	11.75	12.75	13.25	14
Second resonance frequency (Hz)	24.75	26	27.5	28.75
Frequencies ratio	2.11	2.04	2.08	2.05

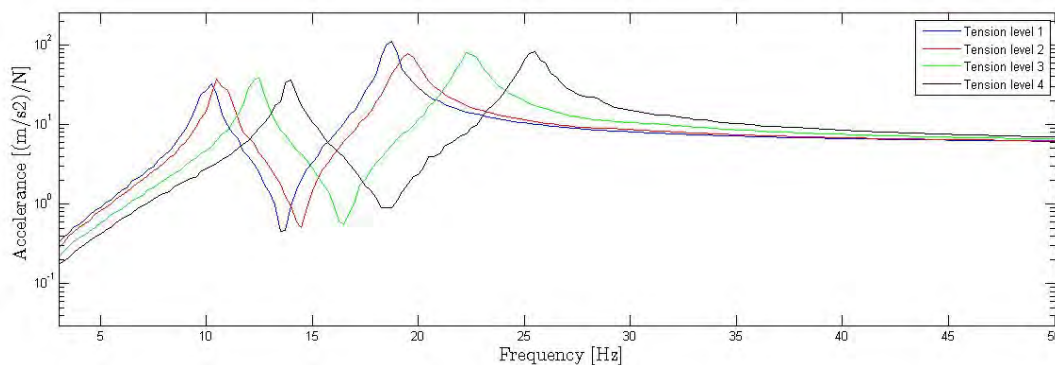


Figure 6. Accelerance FRFs in x coordinate for different wire tension in air - environment.

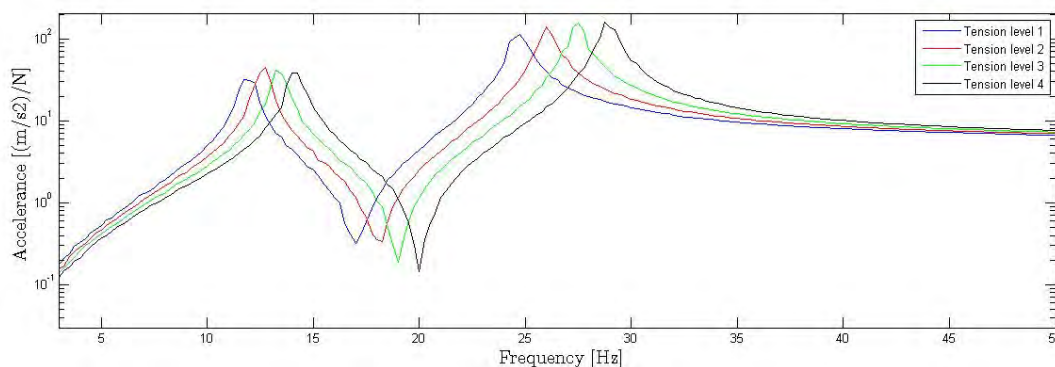


Figure 7. Accelerance FRFs in y coordinate for different wire tension in air - environment.

Once first resonance frequency was tuned, then some tests were carried out to compare x and y FRFs using the same tension level in the wires, a plot is presented in Fig. 8. It shows that the first resonance frequencies values are the same in both cases, which makes sense because of bouncing displacement is the same in x and y coordinates from a mechanical

point of view. This matching did not occur for the second resonance frequencies neither for antiresonances. The difference is due to the fact that during the rocking mode the wire stretching is not the same between x and y excitation cases.

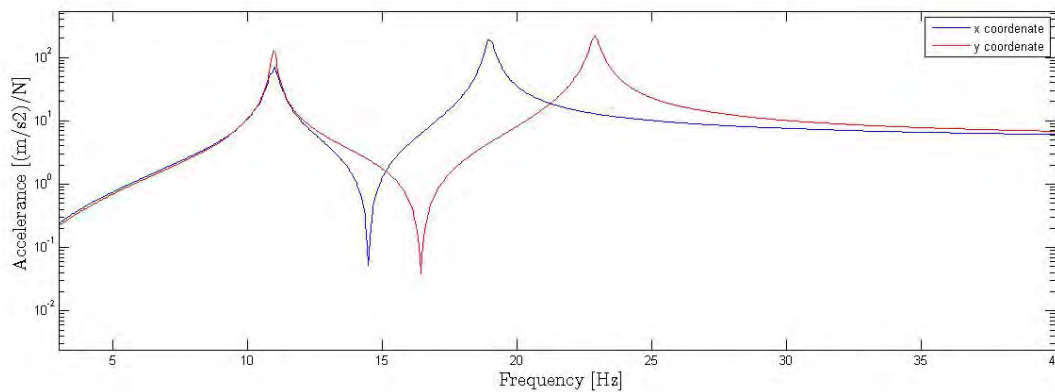


Figure 8. Accelerance FRFs in x and y coordinate for the same wire tension in air - environment.

Subsequently, experiments were performed for x and y excitation separately in air, water and air-water environments. Different multiphase tests were conducted, with air flow values of: 0.27; 0.53; 1; 2.1 and 3.2 [m^3/s] into stagnant water. Resulting FRF plots are presented in Fig. 9 and Fig. 10.

FRF plots of water environment tests show that resonance frequencies change although the tension in wires was maintained the same as used in air environment experiments. This reduction in the resonance frequency of the tube is due to the added mass effect, that corresponds to a surrounding layer of water that moves with the tube. Thus, mass was added to the system but stiffness remain the same, which leads a change of resonance frequencies values, however, the ratio between resonance frequencies in x and y is maintained.

As the turbulent air flow is introduced, the FRFs smoothness is lost. The moving bubbles represent an experimental challenge because as they hit the tube, the distributed load has the same order of magnitude as the shaker input force, which leads to corrupted FRF measurement. The effect of the additional excitation on the FRF estimation can also be noticed when analysing the Coherence Functions (Figs. 9(b) and 10(b)). The relevance of the distributed load (which cannot be measured) leads to low Coherence between the output accelerations and the single force input. If the shaker input force could be increased, the quality of the FRFs would increase, but it is clear one can easily reach the shaker maximum force of, even, overload the impedance head. Therefore, the results corresponding to the higher air flows should be interpreted with care. Anyway, despite this problem, all multiphase FRF plots appear below the water environment FRF, which is an interesting feature as the dynamic system does not show any important shift of resonance frequencies when the bubbles are present.

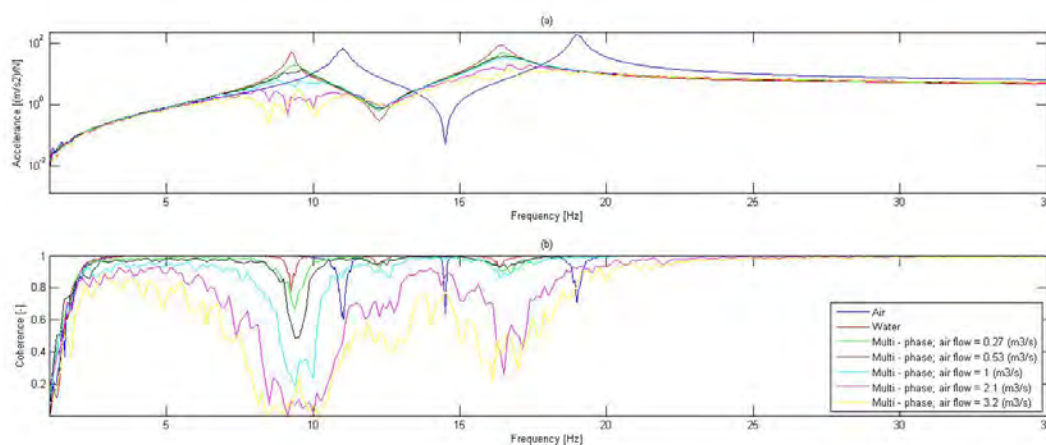


Figure 9. Vibration test in x coordinate for different environments.(a) Accelerance FRFs. (b) Coherence functions.

4. SYSTEM DYNAMIC MODEL

In order to understand the behavior of the dynamic structure detailed above, a model was developed to be compared with the experimental results of the dynamic structure tuned in 11 Hz. Due to the fact that the higher resonance frequency

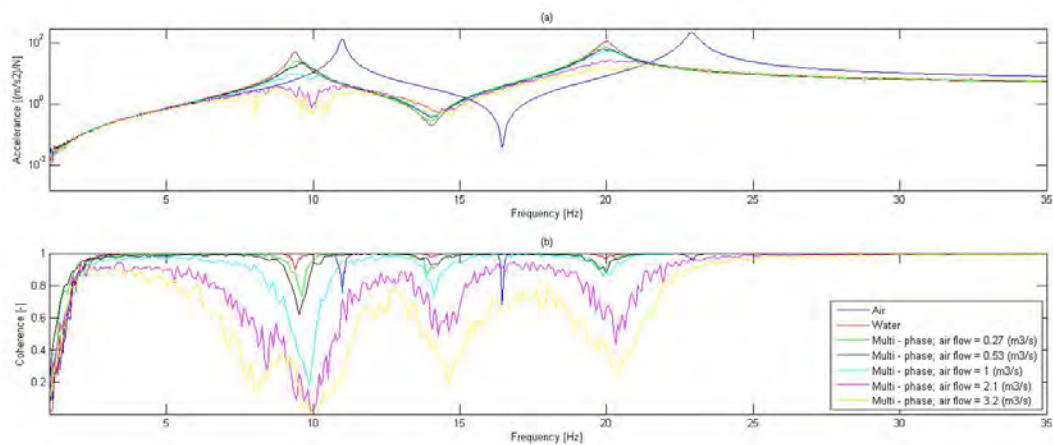


Figure 10. Vibration test in y coordinate for different environments.(a) Accelerance FRFs. (b) Coherence functions.

of the tuned system was 22.9 Hz and no other resonance (apart from the first) appeared in the 0 - 256 Hz frequency bandwidth (the highest resonance frequency is lower than 10% of the higher limit of the bandwidth of interest), then continuous beam vibration modes were not considered in this analysis. The development of the model was done based on the system schematically presented in Fig. 11. Khalifa (2012) presents a similar formulation for one wire by side.

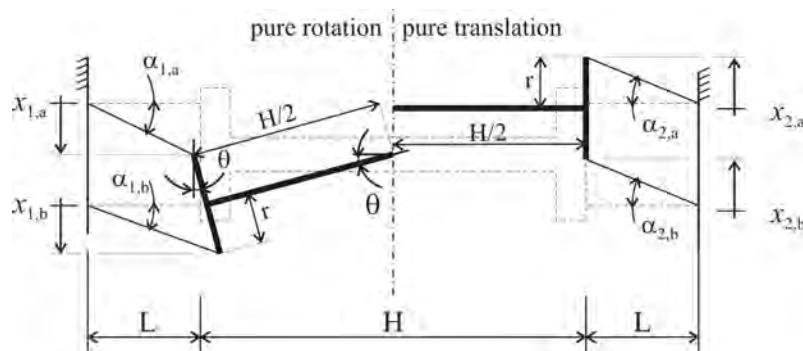


Figure 11. Tube displacement coordinates and parameters

By considering just bouncing and rocking vibration modes and using the Newton's laws the equations of motion of the system can be derived. First, for pure translation mode Eq. (1) can be proposed:

$$\Sigma F_x = m\ddot{x}_c = -4T\sin\alpha, \quad (1)$$

where m is equal to the mass of the rigid body assembly, T is the tension in the wires. x_c is the mid-point displacement of the tube and α is the angle formed by the wire and the horizontal reference as can be seen in Fig. 11. In pure translation case α can be considered equal for the four wires ($\alpha = \alpha_{1,a} = \alpha_{1,b} = \alpha_{2,a} = \alpha_{2,b}$). Considering small angles:

$$\tan\alpha \approx \sin\alpha \approx \alpha \approx \frac{x_c}{L} \quad (2)$$

By using this expression, Eq. (1) can be linearized resulting in Eq. (3).

$$m\ddot{x}_c + \left(\frac{4T}{L}\right)x_c = 0 \quad (3)$$

As it can be seen on the left - hand side in Fig. 11 (pure rotation) there is no symmetry between the two adjacent wires. In order to derive the equations of motion, first we write down the equations for the forces acting on each wire:

$$\vec{F}_{1,a} = -T\cos\alpha_{1,a}\vec{i} - T\sin\alpha_{1,a}\vec{j} \quad (4)$$

$$\vec{F}_{1,b} = -T\cos\alpha_{1,b}\vec{i} - T\sin\alpha_{1,b}\vec{j} \quad (5)$$

$$\vec{F}_{2,a} = T\cos\alpha_{2,a}\vec{i} - T\sin\alpha_{2,a}\vec{j} \quad (6)$$

$$\vec{F}_{2,b} = T\cos\alpha_{2,b}\vec{i} - T\sin\alpha_{2,b}\vec{j} \quad (7)$$

In Eqs. (4) to (7) small values of α are expected, then they can be expressed in function of θ :

$$\alpha_{1,a} = \frac{-H\theta}{2(L-r\theta)} \quad (8)$$

$$\alpha_{1,b} = \frac{-H\theta}{2(L+r\theta)} \quad (9)$$

$$\alpha_{2,a} = \frac{H\theta}{2(L+r\theta)} \quad (10)$$

$$\alpha_{2,b} = \frac{H\theta}{2(L-r\theta)} \quad (11)$$

The lever arm vectors are defined in the next equations. The center of gravity of the tube is used as the reference.

$$\vec{r}_{1,a} = \left(-\frac{H}{2} - r\theta\right) \vec{i} + \left(-\frac{H}{2}\theta + r\right) \vec{j} \quad (12)$$

$$\vec{r}_{1,b} = \left(-\frac{H}{2} + r\theta\right) \vec{i} + \left(-\frac{H}{2}\theta - r\right) \vec{j} \quad (13)$$

$$\vec{r}_{2,a} = \left(\frac{H}{2} - r\theta\right) \vec{i} + \left(\frac{H}{2}\theta + r\right) \vec{j} \quad (14)$$

$$\vec{r}_{2,b} = \left(\frac{H}{2} + r\theta\right) \vec{i} + \left(\frac{H}{2}\theta - r\right) \vec{j} \quad (15)$$

Then, four moments can be calculated by the well - known formula shown in Eq. (16).

$$\vec{M} = \left(\vec{r} \times \vec{F}\right) \quad (16)$$

All those moments are perpendicular to the paper plane. The sum of them must be equal to the rotational inertia of the system:

$$\Sigma M = I_0 \ddot{\theta} \quad (17)$$

After some algebraic operations Eq. (18) is obtained, which is the expression for the system angular displacement.

$$I_0 \ddot{\theta} + THL(H+2L) \left(\frac{\theta}{L^2 - r^2\theta^2}\right) = 0 \quad (18)$$

As can be noticed from Eq. (18), there is a non - linear term in function of θ . Since low values are expected for θ , then $r^2\theta^2$ can be considered as a negligible term. Therefore Eq. (18) can be expressed as:

$$I_0 \ddot{\theta} + \frac{TH(H+2L)}{L} \theta = 0 \quad (19)$$

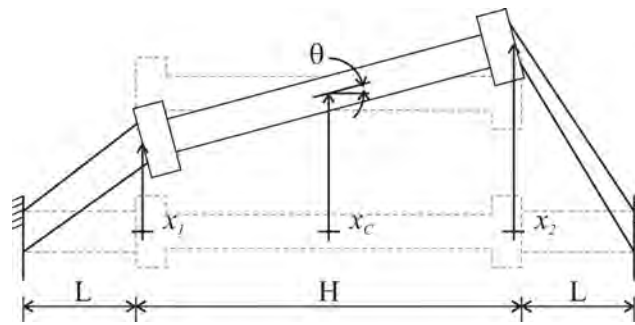
By combining Eqs. (3) and (19), the superposition of translation and rotation can be combined in the system of linear differential equations represented in a matrix form in Eq. (20) and synthesized in Eq. (21). The independent variables of this system are x_c and θ .

$$\begin{bmatrix} m & 0 \\ 0 & I_0 \end{bmatrix} \begin{bmatrix} \ddot{x}_c \\ \ddot{\theta} \end{bmatrix} + \begin{bmatrix} \frac{4T}{L} & 0 \\ 0 & \frac{TH(H+2L)}{L} \end{bmatrix} \begin{bmatrix} x_c \\ \theta \end{bmatrix} = \begin{bmatrix} 0 \\ 0 \end{bmatrix} \quad (20)$$

$$[M] [\ddot{x}] + [K] [x] = 0 \quad (21)$$

From experimental and practical points of view, is more interesting to express Eq. (20) in an alternative coordinate system x' that uses the tube ends displacements x_1 and x_2 . This can be done, for this two-degree of freedom system, by multiplying Eq. (21) by a matrix of transformation based on the system geometry. Eq. (22) and Eq. (23) can be derived from Fig. 12.

$$\theta_c = \left(\frac{-1}{L}\right) x_1 + \left(\frac{1}{L}\right) x_2 \quad (22)$$

Figure 12. Coordinate system $x_c - \theta$ and $x_1 - x_2$

$$x_c = \left(\frac{1}{2}\right)x_1 + \left(\frac{1}{2}\right)x_2 \quad (23)$$

The matrix for linear transformation T_c is composed by Eq. (21) and Eq. (22).

$$T_c = \begin{bmatrix} \frac{1}{2} & \frac{1}{2} \\ -\frac{1}{H} & \frac{1}{H} \end{bmatrix}$$

Thus, Eq. (21) can be modified by T_c to express the system in an alternative coordinate system x' as follows:

$$[T_c]^t [M] [T_c] [\ddot{x}'] + [T_c]^t [K] [T_c] [x'] = 0 \quad (24)$$

Finally, the system of differential equations of Eq. (20) can be expressed as:

$$\begin{bmatrix} \frac{m}{4} + \frac{I_0}{H^2} & \frac{m}{4} - \frac{I_0}{H^2} \\ \frac{m}{4} - \frac{I_0}{H^2} & \frac{m}{4} + \frac{I_0}{H^2} \end{bmatrix} \begin{bmatrix} \ddot{x}_1 \\ \ddot{x}_2 \end{bmatrix} + \begin{bmatrix} \frac{2T(H+L)}{HL} & \frac{-2T}{H} \\ \frac{-2T}{H} & \frac{2T(H+L)}{HL} \end{bmatrix} \begin{bmatrix} x_1 \\ x_2 \end{bmatrix} = \begin{bmatrix} 0 \\ 0 \end{bmatrix} \quad (25)$$

The values used for the parameters in Eq. (25) are presented in Tab. 3. Due to the fact that the tension in the wires were not measured, they were calculated using Eq. (3) and Eq. (18), and damped frequencies were obtained from experimental results. The damping ratios were calculated from experimental results by using the Nyquist method. Previously, the Eigensystem Realization Algorithm (ERA) technique was used to generate the Nyquist plots, results are presented in Tab. 4. Theoretical and experimental FRFs for air environment are compared in Fig. 13 and Fig. 14 for x and y coordinates respectively. As it can be noticed experimental and theoretical FRFs are in good agreement for the two frequency resonances in x coordinate and the first frequency resonance in y coordinate. The second frequency resonance of the theoretical FRF in y coordinate does not agree with the experimental results, which would be related with the linearization in Eq. (19).

Table 3. Model parameters and dimensions values

Symbol	Unit	Value
m	kg	0.482
L	m	0.165
r	m	0.013
I_0	kg m ²	0.0131
H	m	0.43
T (calculated)	N	95

Table 4. Damping ratio values

Coordinate	Mode 1	Mode 2
x	0.014	0.008
y	0.00635	0.006944

5. CONCLUSIONS

The current paper has reviewed some systems used to suspend a tube in a test bench for FIV studies. The use of a dynamic structure composed basically by tensioned wires is a feasible option since it is a relatively simple mechanism

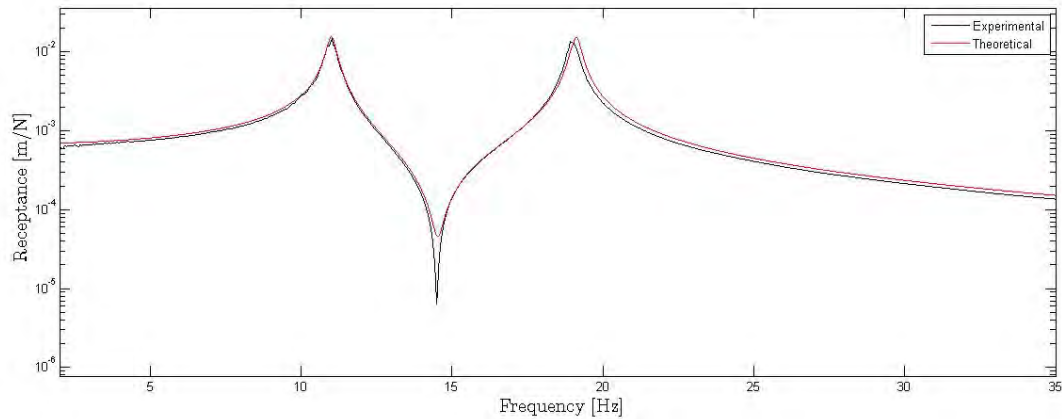


Figure 13. Experimental and theoretical FRFs in x coordinate in air - environment.

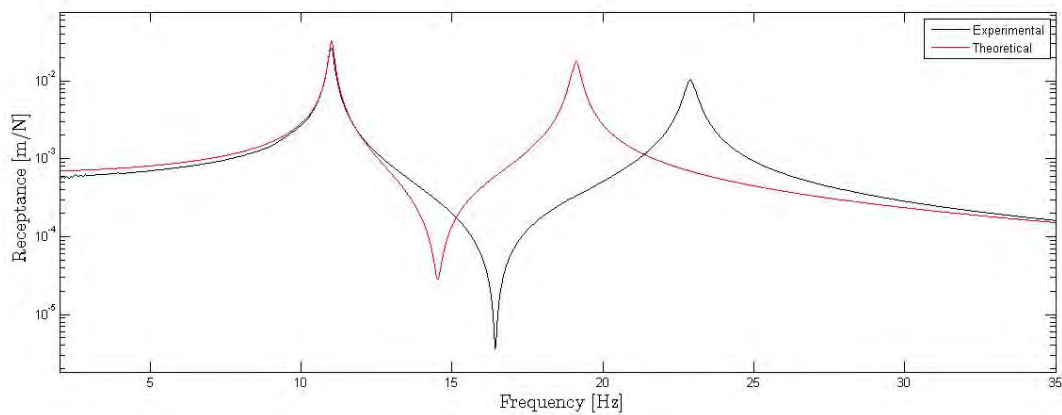


Figure 14. Experimental and theoretical FRFs in y coordinate in air - environment.

that allows the tuning of resonance frequencies.

Theoretical and experimental FRFs are in good agreement for x coordinate, thus, the dynamic model is reliable for vibrations occurring on that direction. On the other hand, for the y coordinate, just the bouncing mode can be well predicted. This effect is related with wire unequal stretching in rocking mode.

As expected, the two first vibration modes of the system are bouncing and rocking. It is important to maintain these modes far away from the first bending mode resonance frequency, thus avoiding mode attachment and, therefore, allowing the dynamic structure to be modeled as a two-degree of freedom system with only rigid-body vibration modes.

When two parallel wires are used as flexible suspension elements, as in the current case, the first resonance frequency is the same for x and y coordinates, however, the second resonance frequencies in each direction are different. This must be related with the different kind of displacements that occur in x and y rocking mode and the difference in wire stretching conditions for each case. This feature could be interesting from a point of view, as excitation in each direction could be more easily detected by observing each frequency range separately, however, the intrinsic geometric nonlinearity provided by the parallel wire approach (Eqs. 4 - 7) could burden the very same procedure. Current studies are focused on addressing these issues.

Good damping ratio approximations are obtained for this system by using the Nyquist method. The ERA technique is very useful to generate good quality Nyquist plots. The next steps regarding damping estimation are focused on identifying a relationship between added damping and void fraction and checking if the ERA technique remains suitable for multiphase condition.

It was possible to observe that for FRFs measured in air - water environment, the higher the air flow the worse the FRF quality. FRFs bad quality is related with the difficulty of measuring distributed force exerted by the bubbles over the

22nd International Congress of Mechanical Engineering (COBEM 2013)
November 3-7, 2013, Ribeirão Preto, SP, Brazil

tube. In spite of this fact, it was seen that the FRFs overall level always appeared below the pure water environment FRFs, which means that great behaviour changes are not expected under multiphase environment case.

Finally, a different suspension configuration, which is axially symmetric with respect to the tube, is under development. The two configurations are intended to be tested in the full test bench, under flow excitation in the near future.

6. ACKNOWLEDGEMENTS

The authors acknowledge the financial assistance of Ecuador SENESCYT (Secretaría Nacional de Educación Superior, Ciencia y Tecnología), and the Brazilian National Council for Scientific and Technological Development - CNPq.

7. REFERENCES

- Axisa, F., Antunes, J. and Villard, B., 1990. "Random excitation of heat exchanger tubes by cross - flows". *Journal of Fluids and Structures*, Vol. 4, pp. 321 – 341.
- Blevins, R.D., 1977. *Flow induced vibration*. Van Nostrand Reinhold, New York, 1st edition.
- Goyder, H.G.D., 2002. "Flow - induced vibration in heat exchangers". *Trans IChemE*, Vol. 80, p. Part A.
- Grover, L.K. and Weaver, D.S., 1978. "Cross - flow induced vibrations in a tube bank - vortex shedding". *Journal of Sound and Vibration*, Vol. 59(2), pp. 263 – 276.
- Khalifa, A., 2012. *Fluidelastic Instability in Heat Exchanger Tube Arrays*. Ph.D. thesis, McMaster University, Ontario.
- Khushnood, S., Khan, Z.M., Malik, M.A., Koreshi, Z.U. and Khan, M.A., 2004. "A review of heat exchanger tube bundle vibrations in two - phase cross - flow". *Nuclear Engineering and Design*, Vol. 230, pp. 233 – 251.
- Paidoussis, M.P., 1982. "A review of flow - induced vibrations in reactors and reactor components". *Nuclear Engineering and Design*, Vol. 74, pp. 31 – 60.
- Pettigrew, M.J., Taylor, C.E. and Kim, B.S., 2001. "The effects of bundle geometry on heat exchanger vibration in two - phase cross - flow". *Journal of Pressure Vessel Technology*, Vol. 123, pp. 414 – 420.
- Price, S.J., Paidoussis, M.P., Macdonald, R. and Mark, B., 1987. "The flow - induced vibration of a single flexible cylinder in a rotated square array of rigid cylinders with pitch-to-diameter ratio of 2.12". *Journal of Fluid and Structures*, Vol. 1, pp. 359 – 378.
- Zhang, C., Mureithini, N.W. and Pettigrew, M.J., 2008. "Development of models correlating vibration excitation forces to dynamic characteristics of two - phase flow". *International Journal of Multiphase Flow*, Vol. 34, pp. 1048 – 1057.

8. RESPONSIBILITY NOTICE

The authors are the only responsible for the printed material included in this paper.